AMERICAN SOCIETY FOR MICROBIOLOGY | Applied and Environmental Microbiology®

ENVIRONMENTAL MICROBIOLOGY

Complex Microbial Communities Drive Iron and Sulfur Cycling in Arctic Fjord Sediments

J. Buongiorno,[a]* L. C. Herbert,[b] L. M. Wehrmann,[b] A. B. Michaud,[c] K. Laufer,[c] H. Røy,[c] B. B. Jørgensen,[c] A. Szynkiewicz,[d] A. Faiia,[d] K. M. Yeager,[e] K. Schindler,[e] K. G. Lloyd[a]

[a]Department of Microbiology, University of Tennessee, Knoxville, Knoxville, Tennessee, USA
[b]School of Marine and Atmospheric Sciences, Stony Brook University, Stony Brook, New York, USA
[c]Center for Geomicrobiology, Department of Bioscience, Aarhus University, Aarhus, Denmark
[d]Department of Earth and Planetary Sciences, University of Tennessee, Knoxville, Knoxville, Tennessee, USA
[e]Department of Earth and Environmental Sciences, University of Kentucky, Lexington, Kentucky, USA

ABSTRACT Glacial retreat is changing biogeochemical cycling in the Arctic, where glacial runoff contributes iron for oceanic shelf primary production. We hypothesize that in Svalbard fjords, microbes catalyze intense iron and sulfur cycling in low-organic-matter sediments. This is because low organic matter limits sulfide generation, allowing iron mobility to the water column instead of precipitation as iron monosulfides. In this study, we tested this with high-depth-resolution 16S rRNA gene libraries in the upper 20 cm at two sites in Van Keulenfjorden, Svalbard. At the site closer to the glaciers, iron-reducing *Desulfuromonadales*, iron-oxidizing *Gallionella* and *Mariprofundus*, and sulfur-oxidizing *Thiotrichales* and *Epsilonproteobacteria* were abundant above a 12-cm depth. Below this depth, the relative abundances of sequences for sulfate-reducing *Desulfobacteraceae* and *Desulfobulbaceae* increased. At the outer station, the switch from iron-cycling clades to sulfate reducers occurred at shallower depths (~5 cm), corresponding to higher sulfate reduction rates. Relatively labile organic matter (shown by $\delta^{13}C$ and C/N ratios) was more abundant at this outer site, and ordination analysis suggested that this affected microbial community structure in surface sediments. Network analysis revealed more correlations between predicted iron- and sulfur-cycling taxa and with uncultured clades proximal to the glacier. Together, these results suggest that complex microbial communities catalyze redox cycling of iron and sulfur, especially closer to the glacier, where sulfate reduction is limited due to low availability of organic matter. Diminished sulfate reduction in upper sediments enables iron to flux into the overlying water, where it may be transported to the shelf.

IMPORTANCE Glacial runoff is a key source of iron for primary production in the Arctic. In the fjords of the Svalbard archipelago, glacial retreat is predicted to stimulate phytoplankton blooms that were previously restricted to outer margins. Decreased sediment delivery and enhanced primary production have been hypothesized to alter sediment biogeochemistry, wherein any free reduced iron that could potentially be delivered to the shelf will instead become buried with sulfide generated through microbial sulfate reduction. We support this hypothesis with sequencing data that showed increases in the relative abundance of sulfate reducing taxa and sulfate reduction rates with increasing distance from the glaciers in Van Keulenfjorden, Svalbard. Community structure was driven by organic geochemistry, suggesting that enhanced input of organic material will stimulate sulfate reduction in interior fjord sediments as glaciers continue to recede.

KEYWORDS Arctic, fjord, iron reducers, microbial communities, sulfate reducers, Svalbard

Citation Buongiorno J, Herbert LC, Wehrmann LM, Michaud AB, Laufer K, Røy H, Jørgensen BB, Szynkiewicz A, Faiia A, Yeager KM, Schindler K, Lloyd KG. 2019. Complex microbial communities drive iron and sulfur cycling in Arctic fjord sediments. Appl Environ Microbiol 85:e00949-19. https://doi.org/10.1128/AEM.00949-19.

Editor Shuang-Jiang Liu, Chinese Academy of Sciences

Address correspondence to K. G. Lloyd, klloyd@utk.edu.

* Present address: J. Buongiorno, Geophysical Laboratory, Carnegie Institute for Science, Washington, DC, USA.

Received 24 April 2019
Accepted 28 April 2019
Accepted manuscript posted online 10 May 2019
Published 1 July 2019

With a warming rate twice the global average, the Arctic is under persistent threat of climate-linked alterations that involve reduced sea ice cover (1, 2) and accelerated glacial retreat (3–6). Glaciers are a major source of iron to offshore environments (7), where it is an important micronutrient for primary producers (8, 9). Highly productive Arctic shelf waters represent a considerable carbon dioxide sink that is predicted to increase with the decline in sea ice cover (10–12). However, models predicting carbon cycle feedbacks in the Arctic have so far not considered the decreased iron delivery to the shelf that might coincide with glacial retreat. Although studies have evaluated the abiotic factors controlling transport and transformation of glacially derived iron in Arctic environments (13, 14), the biological catalysts controlling iron transport have only been hypothesized (14, 15).

In most temperate coastal sediments, microbial dissimilatory iron and sulfate reducers remineralize organic matter to carbon dioxide (16–18). Electron donors for dissimilatory sulfate and iron reduction are H_2, formate, acetate, or other volatile fatty acids produced by microbial fermentation of organic matter (19, 20). This makes the biogeochemical cycling of carbon, iron, and sulfur tightly linked (17). The reduced iron and sulfur that result from these processes form iron monosulfide (FeS) or pyrite (FeS_2), which effectively sequester iron in sediments (21).

In Svalbard, glacially derived iron-rich plumes containing reducible iron (oxyhydr)oxides, as well as detrital pyrites, settle in fjord sediments during seasonal melting (14, 15). Glacial runoff increases turbidity and decreases primary production in fjord waters, resulting in low inputs of fresh organic matter to the sediments (for examples, see reference 22). Low organic matter quality and availability result in low sulfate reduction rates and thus limited sulfide production by sulfate-reducing microbes (14). This removes the pyrite sink for iron and allows reduced iron to be reoxidized either through biomixing or by microbial iron oxidizers (23). Thus, reduced iron can be oxidized either abiotically or via microbial catalysis (24). Reduced iron that evades reoxidation can be transported to the overlying water and potentially transported offshore, where it may stimulate primary production (14).

Despite being permanently cold (2.6 to −1.7°C [25]), Svalbard sediments demonstrate microbial activities (26) and rates of sulfate reduction (27–29) that are comparable to those of temperate sediments. Although the biogeochemical processes have been well described for many Svalbard fjords, studies on the microorganisms that drive them have largely been restricted to Smeerenburgfjorden, which has high organic matter availability and low iron delivery relative to other Svalbard fjords due to the absence of large glaciers in this fjord. Smeerenburgfjorden sediment has 16S rRNA genes (30) and isolates (31) from clades within the genera *Desulfuromusa*, *Desulfuromonas*, *Shewanella*, *Desulfosarcina*, and *Desulfovibrio* capable of sulfate reduction, iron reduction, and sulfur oxidation (sometimes with multiple electron acceptors used by the same isolate). A high diversity of extracellular enzyme targets is paralleled by a high diversity of heterotrophs, demonstrating a robust organic matter-remineralizing community fueled by the removal of fermentative products by iron and sulfur reduction (32, 33). The resulting sulfide and reduced iron largely precipitate as iron monosulfide and pyrite, sequestering them from the water column in this fjord (14).

In contrast to Smeerenburgfjorden, Van Keulenfjorden (Fig. 1) is heavily influenced by iron-rich sandstone and red conglomerate bedrock, resulting in high sedimentary iron accumulation and high water column turbidity that decrease primary production close to the glaciers (for examples, see reference 22). We predict that this geochemical environment supports enhanced iron-mediated recycling of sulfur species close to the glaciers. We further predict that the lower availability of organic matter close to the glaciers results in a diminished role of sulfate reducers, explaining why others (14) have modeled high iron and/or manganese fluxes into the water column rather than iron being sequestered as pyrite. We tested these predictions by comparing the abundances and diversities of likely iron- and sulfur-cycling microorganisms in Van Keulenfjorden sediment at two sites with different proximities to the glaciers.

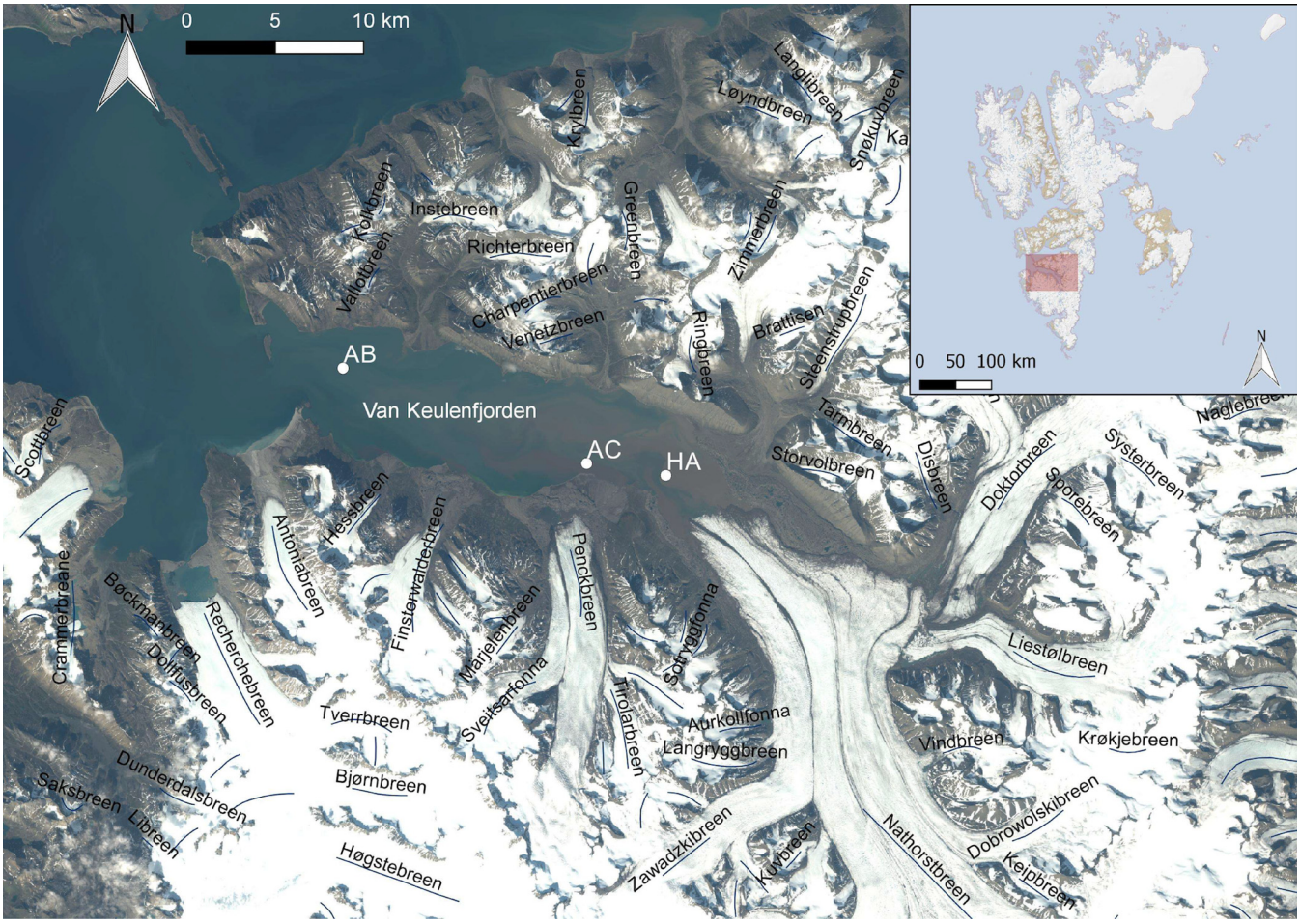

FIG 1 Map of Van Keulenfjorden, Svalbard (red box in inset). Locations of stations are marked along with surrounding glaciers, with detailed 10-m satellite imagery from *Sentinel-2* taken on 2 August 2017.

RESULTS AND DISCUSSION

Sediment characteristics and glacial history. Stations AB, AC, and HA in Van Keulenfjorden were sampled (Fig. 1), with separate cores at each station collected only a few centimeters apart in August 2016. Sediment was dark gray to black, sticky, and fine grained; no sulfide smell was ever detected. Gamma activity was detected for age dating, but non-steady-state input of radioisotopes precluded the use of ^{210}Pb for age dating (see Fig. S1A in the supplemental material). A distinct ^{137}Cs peak at 16 to 17 cm below seafloor (cmbsf), however, indicated the year 1963 (Fig. S1B) (34), giving a mean sediment accumulation rate of 0.31 $\pm$ 0.02 cm year^{-1} over the last ~50 years at station AC. Previous measurements in the area have shown a lower sediment accumulation rate, 0.06 cm year^{-1} (35, 36). The near absence of ^{137}Cs in the top 10 cm indicates that this material either is ancient or has not been exposed to the atmosphere. This layer coincided with a horizon of coarse material, which could have been deposited in a single slump event that created a layer of older material on top of younger sediments. Alternatively, it could represent a deposit of glacial material that has been isolated from the atmosphere.

Porewater iron and manganese. Station HA had the lowest porewater iron concentrations, never exceeding 16 nM (Fig. S2A). Values were similarly low within shallow sediments at station AC, where concentrations remained <70 nM above 12 cmbsf. Below 12 cm, porewater iron concentrations climbed to 658 nM, in line with previously reported elevated porewater iron concentrations for station AC (14). Porewater iron at station AB rose from 24 nM to 227 nM within the first 3 cm and remained fairly steady

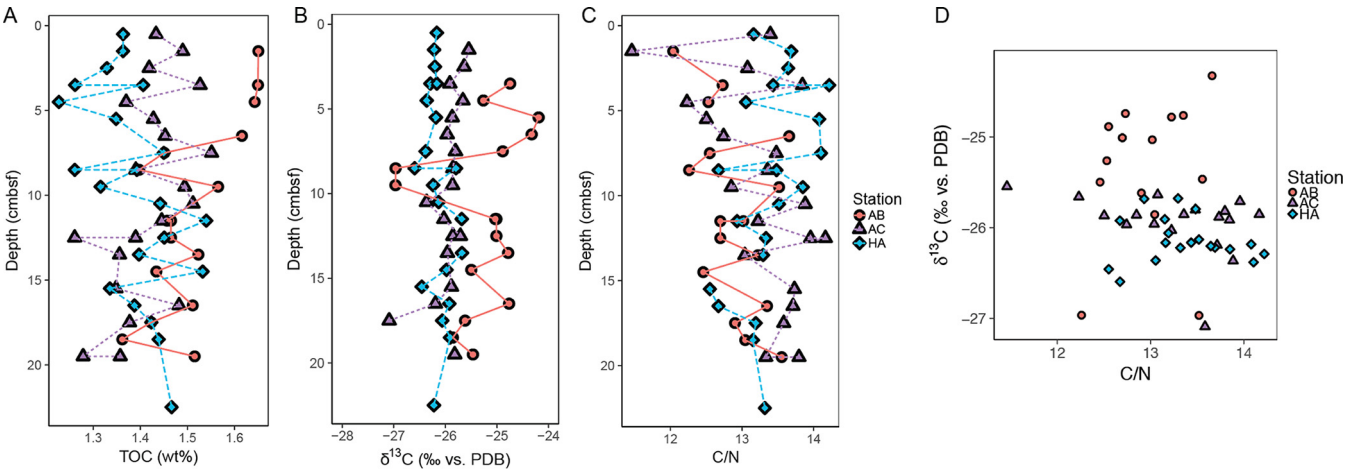

FIG 2 Organic geochemical data. Downcore profiles of total organic carbon (TOC) (A), organic carbon isotopes of bulk organic matter ($\delta^{13}C_{org}$) (B), carbon to nitrogen (C/N) ratios (C), and crossplot analysis for sites AB, AC, and HA (D). All data are reported in Table S1.

downcore, reaching a maximum of 328 nM. Porewater manganese concentrations at station HA were below 50 nM above a 12-cm depth and increased to a maximum of 160 nM at 16.5 cmbsf (Fig. S2B). At the surface at station AC, porewater manganese measured 120 nM and reached a maximum of 253 nM at 4.5 cmbsf. Below this interval, values steadily decreased. At station AB, manganese concentrations remained <66 nM. The elevated concentration of dissolved iron and manganese observed across all stations may result from the combination of dissimilatory metal reduction and the abiotic reduction of iron (oxyhydr)oxides and manganese oxides through cycling of sulfur intermediates generated by microbial reduction of sulfate, the concentrations of which remained steady down to 20 cmbsf (HA, 26.69 to 27.46 mM; AC, 27.20 to 28.01 mM; AB, 27.05 to 28.97 mM [L. C. Herbert, N. Riedinger, A. B. Michaud, K. Laufer, H. Røy, B. B. Jørgensen, C. Heilbrun, R. C. Aller, J. K. Cochran, and L. M. Wehrmann, submitted for publication]).

Organic and isotope geochemistry. Total organic carbon (TOC) values averaged 1.4 wt% ± 0.1 wt% at inner station HA, 1.4 wt% ± 0.1 wt% at middle station AC, and 1.5 wt% ± 0.1 wt% at the outer station AB (Fig. 2A and Table S1). After statistical outliers were removed (Fig. S3) and when all data from each core were combined, TOC was higher at outer station AB than at middle station AC (*P* value of Welsh two-sample *t* test = 0.004) and inner station HA (*P* value of Welsh two-sample *t* test = 0.0002). Low TOC content is typical of Svalbard fjords (14, 37), where sedimentary organic matter is diluted by terrestrial material and turbidity from glacial outflow limits primary production (22).

The average isotope compositions of organic carbon ($\delta^{13}C_{org}$) in Van Keulenfjorden sediment were −26.1‰ ± 0.2‰ at station HA, −26.0‰ ± 0.3‰ at station AC, and −25.3‰ ± 0.8‰ at station AB (Fig. 2B and Table S1). Carbon-to-nitrogen (C/N) ratio averages were 13.4 ± 0.5 at station HA, 13.4 ± 0.5 at station AC, and 12.9 ± 0.5 at station AB (Fig. 2C and Table S1), with an overall average value of ~13.0. The isotope composition of organic matter could be a composite of terrestrially derived coal (average, −26‰) (38), soil (average, −25‰) (38), C_3 land plants (−25 to −35‰) (39), and marine-derived phytoplankton (−22 to −25‰) (40). The highest isotope compositions were identified at station AB, with values as high as −24.1‰. This indicates that a potentially higher fraction of labile, marine phytoplankton drives station AB isotopes to be heavier than that of the other two stations (Fig. 2D), although the exact proportions of each type are unable to be discerned from these data alone. Like $\delta^{13}C_{org}$, the C/N ratios can be used to identify the relative contribution of marine versus terrestrial sources to organic carbon pools, with C/N ratios of allochthonous, terrestrially derived organic matter typically ~20 and marine-derived organics ~6 (37). There is

general agreement with respect to organic matter source between isotope composition and C/N ratios; however, at station AB, the C/N ratios are greater than average phytoplankton values (40). Larger values may reflect either terrestrially derived organic matter or the preferential removal of nitrogen from bulk organic matter during early diagenesis in the seabed (41). Differences in TOC and $\delta^{13}C_{org}$ between sites are restricted to above 6 to 7 cm (Fig. 2) and confirm the seaward gradient of increased carbon amount and lability along the long axis of the fjord observed previously for this and other nearby fjords (14, 22, 37).

Quantitative PCR. Low DNA extraction yields from station HA sediments precluded quantitative PCR (qPCR) measurements for this station, although the same methods were successful at stations AB and AC. Sediments at HA likely had lower microbial biomasses and/or higher concentrations of PCR inhibitors (e.g., iron). At station AB, average bacterial 16S rRNA gene copy numbers ranged from 1.33×10^{11} 16S rRNA gene copies g of fresh sediment^{-1} at 0 to 1 cmbsf to 1.05×10^{8} at 18 to 19 cmbsf (Fig. 3A and Table S2). Values extrapolated above the standard curve (1×10^{9} copies, black dashed line) may not be accurate but are at least higher than the $\sim 10^{9}$ cells g of sediment^{-1} common in temperate, eutrophic marine sediments (42, 43), even assuming an average of three 16S rRNA gene copies per cell (44). High copy numbers could be due to limitations in absolute quantifications of qPCR (45). However, the high copies of the 16S rRNA gene observed in this study are supported by previous high rRNA recovery from sediments from Hornsund, Svalbard (26), suggesting that rapid redox cycling may provide enough energy to support microbial biomass as high as in organic-rich, sulfidic, temperate marine sediments. Archaeal 16S rRNA gene copy numbers were lower, ranging from a peak of 3.9×10^{8} 16S rRNA gene copies g of fresh sediment^{-1} at 4 to 5 cmbsf to 7.4×10^{4} 16S rRNA gene copies g of fresh sediment^{-1} at 18 to 19 cmbsf at station AB (Fig. 3B), in agreement with Smeerenburgfjorden archaeal qPCR measurements (46). The 16S rRNA gene copy numbers at the outer station AB decreased as a function of depth (Table S3) and were higher than for station AC, perhaps reflecting the higher quality and quantity in organic matter here. The large downcore variability in 16S rRNA gene copy numbers at middle station AC was likely not due to experimental error, since replicate measurements were not statistically significantly different (P value of Student's paired t test ≥ 0.1) but instead may have resulted from physical processes that disrupt sediment communities and prokaryote abundance closer to the glaciers, such as highly episodic deposition of sediments with meltwater plumes (47), bioturbation (27, 48), and glacial surge events (35).

Community composition. After normalization, we generated a total of 52 libraries across the two stations that produced amplifiable DNA (e.g., AB and AC [Table S4]). Station HA DNA extraction yields were too low for sequencing. Rarefaction profiles of 16S rRNA gene sequences did not approach a plateau (Fig. S4), suggesting that rare sequences may have been missed in these sediments. Therefore, we interpreted the distribution and co-occurrence patters of only the most abundant sequences. Across all libraries, bacteria comprised the majority of reads (96 to 97% versus archaea at 3 to 4%), in agreement with qPCR. Most sequences (~25% to 42%) belonged to the *Proteobacteria* phylum (Fig. S5). The next most abundant phylum, *Planctomycetes* (~10 to 20%), remained steady downcore at both stations compared to other phyla, such as *Bacteroidetes*. Sequences from *Bacteroidetes* decreased from 16% in surface sediments to 3% relative abundance at both stations, likely due to oxygen limitation in the anoxic sediments.

Community composition across all samples was described mainly by the variability of C/N ratios, $\delta^{13}C_{org}$, and depth, suggesting vertical stratification of sediment communities (Spearman correlation = 0.18). Marginal effects between these variables were not significant ($P > 0.05$), indicating independence between factors. Nonmetric multidimensional scaling (NMDS) analysis showed overall good correspondence in community composition between depth intervals from the same site from different cores (Fig. 4). Compositional differences between sites were largely explained by C/N ratio and

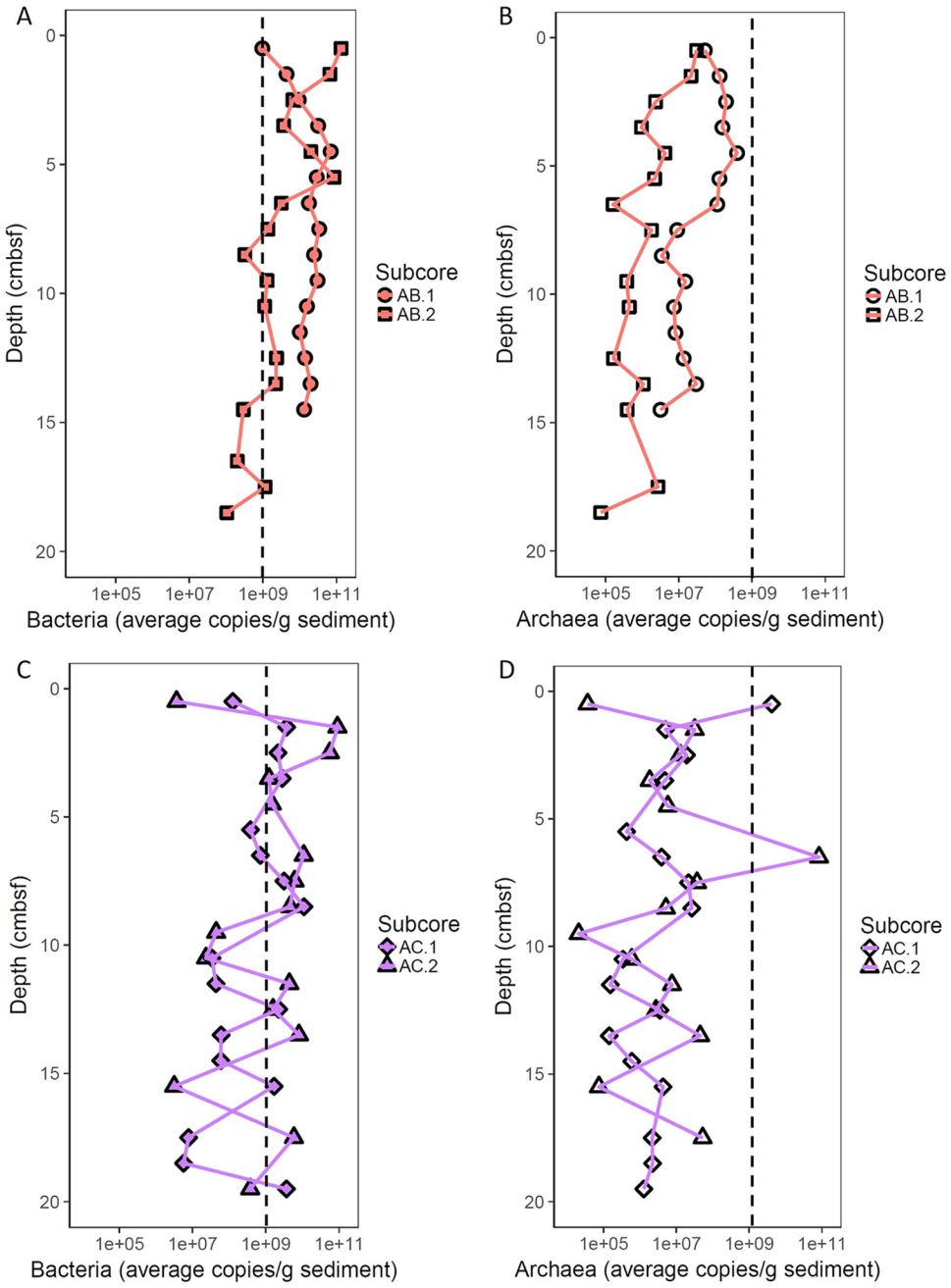

FIG 3 Downcore abundance of the 16S rRNA gene for bacteria (A and C) and archaea (B and D). Average values between technical duplicates are shown for cores AB and AC. All values are reported in Table S2. The dashed line indicates extrapolated values modeled beyond the standard curve.

TOC, which separated shallow AC and AB communities from each other in ordination space (Fig. 4). Samples deeper than 7.5 cm at AB and 10.5 cm at AC converged together toward $\delta^{13}C_{org}$ and depth vectors, suggesting that site-to-site differences in communities are restricted mainly to shallow sediments above 7 to 10 cm, where TOC and $\delta^{13}C_{org}$ composition differences between stations were observed (Fig. 2).

At both stations, sequences related to anaerobic bacteria likely participating in *in situ* cycling of iron and sulfur species were present, including the deltaproteobacterial families *Desulfobacteraceae* and *Desulfobulbaceae* (Fig. S6). High *Desulfobacteraceae* relative abundance was shown previously in Smeerenburgfjorden sediment, with the genera *Desulfosarcina*, *Desulfofrigus*, and *Desulfococcus* as the most abundant sulfate

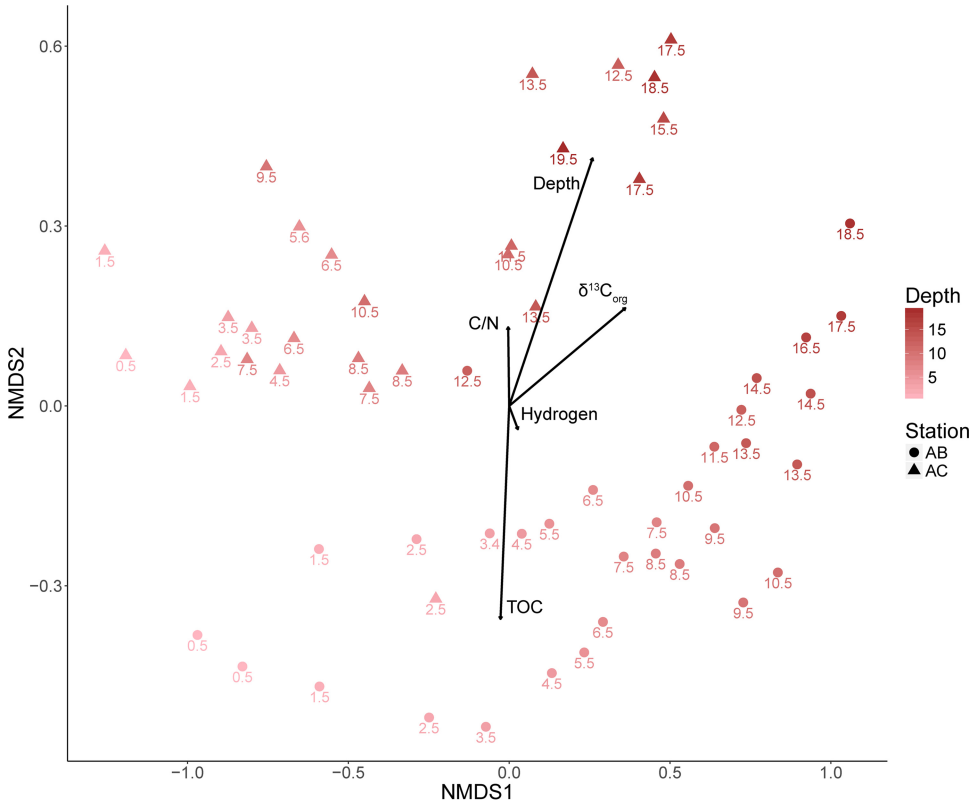

FIG 4 Nonmetric multidimensional scaling (NMDS) plot with environmental and geochemical variables as vectors describing the composition of microbial communities at stations AB and AC.

reducers (30, 49). However, unlike for Smeerenburgfjorden, where *Desulfobulbaceae* were previously not detected, *Desulfobulbaceae* sequences were in high relative abundance in most of our libraries. Sequences related to known sulfate reducers, such as *Desulfococcus* and *Desulfosarcina*, were most abundant within the top 10 cm of the sediment at station AB, while at station AC, their highest abundance occurred deeper, at 17.5 cm (Fig. 5). Members of *Desulfococcus* and *Desulfosarcina* are able to couple the reduction of oxidized sulfur compounds, such as sulfate and sulfite, to the oxidation of volatile fatty acids (50, 51), aromatic compounds (52–54), and H_2 (51, 55). Increases in the relative sequence abundance of *Desulfococcus* and *Desulfosarcina* within uppermost AB sediments coincided with measurements of sulfate reduction rates (SRR), which increased from 3 nmol cm^{-3} day^{-1} within the top 2 cm to 53 nmol cm^{-3} day^{-1} at 2.5 cmbsf (Fig. S7A). The lack of replicate measurements prevents us from assigning too much importance to the 2.5-cm interval; however, the observation that sediments above 5 cm at station AB have some of the highest TOC concentrations (Fig. 2A) suggests that organic electron donors were sufficient to stimulate sulfate reduction at these shallow depths. Directly below this interval, SRR dropped to ~20 nmol cm^{-3} day^{-1} and continued to decline with depth to 9 nmol cm^{-3} day^{-1} at 14.5 cmbsf. Like station AB, SRR at station AC was lowest in the uppermost sediment layers. However, SRR remained low throughout most of the core (<10 nmol cm^{-3} day^{-1} [Fig. S7B]) and the maximum value was observed deep in the core at 18.5 cmbsf (19 ± 25 nmol cm^{-3} day^{-1}).

The trend of increased sulfate reduction beyond 14.5 cm is complicated by inconsistent replicate measurements, suggesting that there is heterogeneity in the distribution of organic electron donors or H_2 at station AC. Support for such heterogeneity comes from H_2 concentrations, which were low throughout most of the AC core, only exceeding 0.8 nM past a 15-cm depth (Fig. S7C). If H_2 is a significant electron donor for sulfate reduction in these sediments, fueling sulfate reducers like Sva0081 sediment

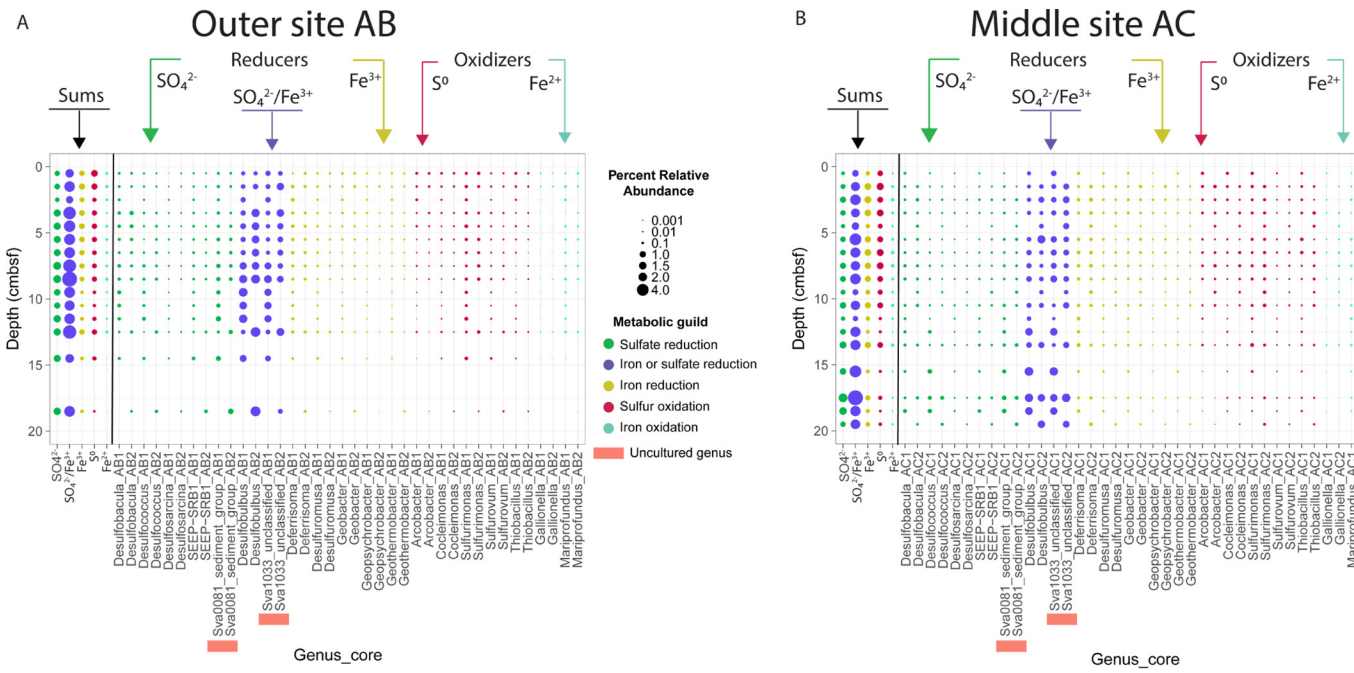

FIG 5 Relative abundances of 16S rRNA gene sequences of taxa of interest at stations AB (A) and AC (B). Sequences are sorted by predicted metabolic guild: sulfate reducers, sulfate/iron reducers, iron reducers, sulfur oxidizers, and iron oxidizers. Uncultured genera for which we predict metabolism are marked with a pink bar. The number next to the genus name on the *x* axis indicates which core the sequences are from. See text for discussion about metabolic plasticity and the use of multiple electron acceptors across these clades.

group which has been suggested through metagenomic and single cell genome analysis to be an important scavenger of H_2 in marine sediments (56), then an SRR above a 15-cm depth at AC was perhaps suppressed by limited availability of H_2. Concentrations of H_2 could be kept low by active microbial iron reduction supported by a pool of highly reactive, bioavailable iron, which has been suggested for another western Svalbard fjord (K. Laufer, A. B. Michaud, H. Røy, and B. B. Jørgensen, submitted for publication).

Suppression of shallow sulfate reduction is supported by sequence data, which showed that taxa capable of sulfate reduction using H_2 at station AC increased from <0.2% at the surface to >5% at 17.5 cm at the expense of sequences related to iron reducers, including the *Desulfuromonadales* (genera *Desulfuromusa, Geopsychrobacter*, *Geothermobacter*, and *Geobacter*) (Fig. 5B). *Geobacteraceae* were less abundant in shallow depths (~5 cmbsf [Fig. 5A]) at station AB than at station AC (~15 cmbsf [Fig. 5B]). *Geobacteraceae* contain numerous adaptations that allow them to thrive in iron-rich anoxic marine sediments, including the ability to oxidize common fermentation products and H_2 while reducing Fe(III) or Mn(IV) (57, 58). The distribution of iron reducers like *Geobacteraceae* may be driven by differences in iron reactivity between the middle and outer sites that cause rapid exhaustion of reactive Fe(III) at station AB. Previous studies have shown that iron reactivity increases farther from glacial inputs, either because the initial iron deposited is more reactive or because reactivity increases with postdepositional reworking (14). So although outer station AB has a lower iron accumulation rate (14), the iron that is deposited here may be more reactive than at middle station AC, permitting spatial differences in iron accumulation and bioavailability to play important roles in biogeochemical cycling of iron and sulfur in Van Keulenfjorden, which has been noted within nearby Van Mijenfjorden (15).

The relative shoaling of the zone of potential sulfate reducers at station AB compared to station AC may be driven by the combination of microbial removal of highly reactive Fe(III) discussed above and the formation of iron monosulfides from sulfide generated by microbial sulfate reduction (59). Vertical zonation between sequences

related to iron reducers and those related to sulfate reducers agrees with thermodynamic sorting based upon energy yield of reduction with Fe(III) and sulfur species (60, 61). However, recent studies have shown that the distribution of iron-reducing bacteria is decoupled from traditional geochemical zonation in sediments and may be driven instead by microniche distribution and metabolic flexibility (62). In fact, the relative read abundance for *Desulfuromusa* displayed no observable trend with depth, perhaps because of the potential to use different electron acceptors experienced with depth, including Fe(III), Mn(IV), elemental sulfur, and nitrate (57, 63). Likewise, *Desulfobulbus* sequences did not show strong vertical sorting at either site but instead were highly abundant at both stations and only slightly increased with depth at AC (Fig. 5). The metabolic diversity of *Desulfobulbus*, including dissimilatory iron reduction (64), oxidation of elemental sulfur (65), sulfur disproportionation (66), and sulfate and sulfite reduction in the complete oxidation of organic matter (67), may allow *Desulfobulbus* to continue to use sulfate or other electron acceptors for growth after the exhaustion of highly reactive Fe(III) at ~5 cm at AB and ~10 cm at AC. This further highlights the potential for multiple controls on microbial distribution in the sediment.

Like *Desulfobulbus*, the Sva1033 sediment group had high sequence abundance at most depths, with little systematic variation downcore at either site. Sva1033 is an uncultured genus of the *Desulfuromondales*, first identified through 16S rRNA gene clone libraries of Smeerenburgfjorden sediment (29). Its closest relative by 16S rRNA gene identity (93.7%) is *Desulfuromonas palmitatis*, a dissimilatory iron reducer capable of oxidizing long-chain fatty acids (68). Because Sva1033 remains uncultured, the extent of its metabolic potential remains unknown; however, we hypothesize that it shares a metabolic mode similar to that of *Desulfobulbus* in these sediments and may rely on metabolic switching from metal reduction to sulfate reduction with depth.

Clades related to known sulfur oxidizers were also present at both sites but were more abundant at station AC. Sequences for *Arcobacter*, *Sulfurimonas*, and *Sulfurovum* (*Epsilonproteobacteria*), *Cocleimonas* (*Gammaproteobacteria*), and *Thiobacillus* (*Betaproteobacteria*) all maintained relatively high sequence abundance with depth at AC (Fig. 5). These groups typically use oxygen or nitrate to oxidize sulfur intermediates, such as thiosulfate and elemental sulfur (69, 70), and therefore rely on abiotic oxidation of sulfide with reducible iron. If reducible iron is found deeper in station AC sediment, redox conditions remain suboxic, and a cryptic iron-sulfur cycle replenishes sulfur intermediates (15, 71). Thus, cryptic iron-sulfur cycling at station AC could provide a consistent source of sulfur intermediates that are useful in biological sulfur oxidation, while shallow exhaustion of reducible iron at station AB prevents high abundance of these clades. Sulfur intermediates generated from combined biological and abiotic reoxidation of sulfide can be oxidized further to sulfate by microbial sulfur disproportionation by groups like *Desulfocapsa*, which was present at low sequence abundance in our libraries (<0.05%). Together with abiotic transformations, this may explain the conservation of porewater sulfate with depth previously noted within Van Keulenfjorden sediments (14).

Reduced iron can be reoxidized both abiotically, through interactions with oxygen and manganese oxides, and biotically, with microbial iron oxidizers such as *Mariprofundus* and *Gallionella* that use nitrate or oxygen delivered through biomixing. *Mariprofundus* sequences were more abundant and penetrated deeper at station AC, much like their sulfide-oxidizing counterparts (Fig. 5). Inconsistent depth trends of *Mariprofundus* sequences between cores taken at the same site may be related to heterogenous distribution of microniches and electron acceptors that support growth. The two isolates from this group, *Mariprofundus ferrooxydans* and *Mariprofundus micogutta*, oxidize Fe(II) with molecular oxygen under microaerophilic conditions (72–74), making growth of this group contingent upon the presence of low-oxygen microniches that can be generated through bioturbation and bottom-water delivery. Because the penetration of oxygen is likely only millimeters (48), the presence of deep *Mariprofundus* sequences indicates that biomixing plays an important role in delivering oxygen to the subsurface. Like for *Mariprofundus*, *Gallionella* sequences were more abundant at

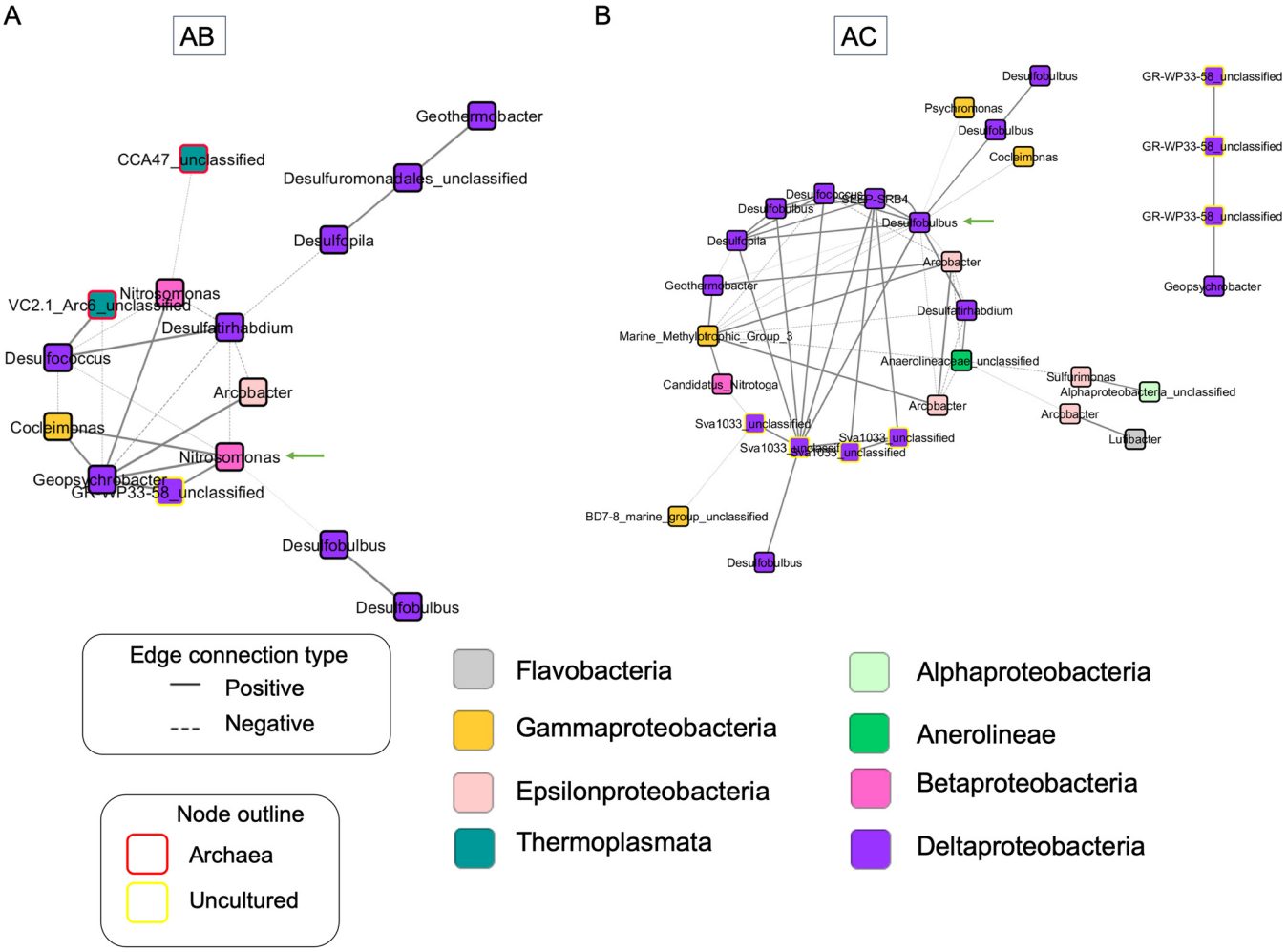

FIG 6 Merged microbial co-occurrence networks. Individual network characteristics have been combined to show merged networks for outer station AB (A) and middle station AC (B) to uncover the core microbiome features at each station. Isolated nodes have been removed for clarity. Each node represents an OTU, with color indicating class-level taxonomy. Genus names are overlaid on each node and edge relationships are indicated with solid and dashed lines for positive and negative connections, respectively. Green arrows indicate the nodes at each site with greatest betweenness.

station AC. However, while *Mariprofundus* sequences extended to 15 cmbsf at AB, *Gallionella* sequences were mostly restricted to the top 2 cm at this station (Fig. 5A). Because station AB is situated near the source of marine waters to the fjord, these observations agree with environmental studies suggesting that *Mariprofundus* is a strict marine iron oxidizer, while *Gallionella* is restricted to freshwater systems or maintains low abundance in marine systems (23, 75).

Microbial networks. In order to investigate potential emergent properties of these complex microbial ecosystems and generate hypotheses about *in situ* interactions, networks were built using the most abundant (top 30) operational taxonomic units (OTUs; 97% similarity) and those OTUs with cultured representatives that cycle iron and/or sulfur. Individual microbial co-occurrence networks were generated for each core (Fig. S8) and then merged to find replicated patterns of co-occurrence between taxa and geochemical data (Fig. 6; cf. reference 76). Neither geochemical data (TOC, $\delta^{13}C_{org}$, C/N, [H_2], [Fe], or [Mn]) nor SRR was found to have a statistically significant relationship with any microbial taxa; instead, connections were limited to interactions between microbial taxa. Therefore, although some of these parameters (e.g., C/N ratios and $\delta^{13}C_{org}$) were correlated with overall microbial community composition (Fig. 4), the variations of these geochemical parameters on a centimeter scale did not drive changes in relative sequence abundances of individual clades.

Deltaproteobacteria from sulfate- and iron-reducing genera were the most common nodes in both the AB and AC networks (8 out of 16 nodes in AB and 11 out of 30 nodes in AC [Table S5]). The AB network contained fewer nodes than the AC network, so it may represent a more stable and established community. The greater taxonomic diversity and larger number of relatively rare-abundance OTUs observed within the AC network may reflect the differences in dissolved nutrients and/or microbial inocula at this station and station AB. Overall, total sequence abundance of an OTU did not dictate the likelihood of being included in a network, and interestingly, the highly abundant group Sva1033 (>1.5% read abundance at both sites) was restricted to the AC network. Here, Sva1033 nodes were connected to a diverse set of *Deltaproteobacteria* (*Desulfococcus*, SEEP-SRB4, *Desulfopila*, and *Desulfobulbus*), each of which was highly connected to other nodes. This suggests that uncultured Sva1033 may have a physiological role (iron or sulfate reduction) similar to those of the cultured groups with which it shares edges at station AC. We tested if relatively rare taxa are important members of the community at each site by calculating betweenness centrality, or average number of shortest paths, for each networked OTU. The betweenness centrality metric can be used to identify key members of a microbial community and help generate hypotheses about the functional role of these microorganisms *in situ* (77). At station AB, a relatively low-abundance *Nitrosomonas* OTU had the highest betweenness centrality (Fig. 6A, green arrow). Members of the *Nitrosomonas* are chemolithoautotrophs that gain energy through the oxidation of ammonia to nitrate (78) and are crucial nitrogen cyclers in marine sediments (79–81). Nitrate generated by *Nitrosomonas* could perhaps benefit members of the community that rely on nitrate for their metabolism, such as iron or sulfur oxidizers, allowing this relatively rare OTU to impart control on co-occurrence patterns between other taxa. At station AC, a *Desulfobulbus* OTU had the highest betweenness centrality (Fig. 6B, green arrow) and the most connections with other taxa, suggesting that this OTU represents a "hub" that connects many nodes that are not directly connected to each other (82). Future work should explore the *in situ* metabolic activity of *Desulfobulbus* in these sediments using incubation approaches, targeted genomics, and/or metabolomics to identify any potential syntrophic interactions with microbial counterparts.

Our network results suggest that intrinsic structure of microbial communities between sites would perhaps be overlooked if sequence abundance was evaluated alone. Together these network results suggest site-specific co-occurrence patterns for the same OTUs, supporting the idea that distance from the glacier was a controlling factor on interactions between microbial taxa, even at high taxonomic resolution. This could be due to differences in environmental controls that foster microbial competition (83) and/or cross-feeding (84).

Conclusions. Our study sheds light on the biological catalysts controlling iron cycling and ultimately transport to the open ocean along western Svalbard. We predict that the growth of sulfate reducers like *Desulfobacteraceae* and *Desulfobulbaceae* will be stimulated in shallow sediments as glaciers continue to recede and sedimentary TOC becomes more plentiful closer to the head of Van Keulenfjorden. The sulfide generated by microbial sulfate reduction can become reoxidized by sulfur oxidizers, such as *Thiobacillus* or *Sulfurimonas*. However, should microbial sulfate reduction outpace microbial sulfur oxidation, excess sulfide will precipitate with reduced iron to form iron sulfide minerals, decreasing the amount of iron being transported to the shelf. Decreased overall export of reduced iron may impact primary production along the shelf, where removal of this key micronutrient could decrease phytoplankton populations that represent a large sink for carbon dioxide in the atmosphere.

MATERIALS AND METHODS

Sample collection. Cores from stations AB, AC, and HA in Van Keulenfjorden were collected in August 2016. Polycarbonate core liners were used to subsample Haps corers (KC Denmark A/S) (85) at each site, with each core (e.g., AB.1, AB.2, and AB.3 at site AB) taken centimeters apart, down to a depth of ~20 cmbsf. Cores were stored at 4°C until they were ready for processing within 8 h. A metal plate and collar were used to collect sediment samples at 1-cm intervals. Cores destined for molecular work (AB.1,

AB.2, AC.1, and AC.2) were processed sterilely outside, where air temperatures remained near *in situ* temperatures (~4°C). Cores for organic and isotope analyses and H_2 (HA.3, AB.3, and AC.3) were processed inside the Kings Bay Marine Lab at room temperature. SRR samples were maintained at low temperature. Sediment samples for organic geochemistry and 16S rRNA gene analysis were stored at −80°C until processed.

Sedimentation accumulation rate. Frozen sediment was shipped on dry ice to University of Kentucky for analysis of natural and anthropogenic gamma emitters via low-level gamma spectroscopy. Sediment accumulation was then calculated from the depth where the maximum activity of ^{137}Cs was found, divided by the time since 1963. This model assumes limited vertical mobility of cesium in sediments (86–88).

Porewater iron and manganese. Values of porewater Fe and Mn originate from different cores from the same station taken during the same campaign in predrilled plastic core liners with a gravity corer device. Porewater was collected anoxically using Rhizon samplers and attached syringes (89, 90). Porewater aliquots for trace metal analysis were separated using plastic syringes and preserved in small Nalgene bottles with trace-metal-grade nitric acid (2% [vol/vol]). Measurements were made at Oklahoma State University in Stillwater, OK, using a Thermo Fisher iCAP Qc inductively coupled plasma-mass spectrometer (ICP-MS). Standards were made to match the porewater matrix by adding the appropriate amount of sodium chloride. Samples were diluted with trace-metal-grade nitric acid and analyzed in random order, along with a standard reference solution (NIST SRM 1643f). Based on the NIST standard which was measured at least 3 times per run, the analytical precision of the porewater analysis was better than 5%. Where data were missing for network analysis, we used averages between adjacent depths.

Organic and isotope geochemistry. Sediment for analysis of organic matter was freeze-dried after thawing from −80°C and subjected to acid fumigation overnight before analysis (91). Total organic carbon (TOC) and isotope compositions of carbon and nitrogen (C/N) from bulk organic matter were measured using a Thermo-Finnigan Delta XL mass spectrometer coupled to an elemental analyzer at the University of Tennessee, Knoxville. C/N ratios were calculated by dividing percent C by percent N. Isotopic values were calibrated against the USGS40 and USGS41 international standards. In-house standard sets were run every 12 samples. Outliers were determined using Cook's distance (92) in R (93). Across multiple runs, 1 standard deviation was 0.1 to 0.2‰ for $\delta^{13}C_{org}$, 1.1 to 1.8% for N, and 1.0 to 2.2% for C.

Quantitative PCR. Genomic DNA was extracted from approximately 2 g of Svalbard sediment per depth using the RNeasy Power Soil kit for RNA extraction with the DNA accessory kit (Qiagen, Valencia, CA). DNA extracts were stored at −80°C until required. We tested 1:1 dilutions and 1:40 dilutions to identify the most suitable concentrations of DNA for qPCR but found that undiluted DNA extracts provided the lowest threshold cycle (C_T) values. Total 16S rRNA gene copy numbers of bacteria and archaea were quantified with qPCR using domain-specific primers. The sequences for the bacterial primer pair Bac340f/Bac515r were 5′-TCCTACGGGAGGCAGCAGT-3′ for the forward primer and 5′-GGACTACCA GGGTATCTAATCCTGTT-3′ for the reverse primer (94). The sequences for the archaeal primer pair Arch806f/Arch915r were 5′-ATTAGATACCCSBGTAGTCC-3′ (where S is either G or C and B is either C, G, or T) for the forward primer and 5′-GTGCTCCCCCGCCAATTCCT-3′ for the reverse primer (95, 96). Extracted DNA was amplified with a Bio-Rad DNA Engine Option 2 system (Applied Biosystems, Foster City, CA) using SYBR green chemistry (Invitrogen master mix). Serial dilutions of extracted plasmids containing amplified partial 16S rRNA genes were used as standards for bacteria and archaea, ranging from 10^2 to 10^9 copies/μl. Nuclease-free water was used as a negative control and undiluted DNA extracts were used as templates. Results of qPCR were rejected if the R^2 of the standard curve was below 0.95 or if there was evidence of primer dimers within the melt curve. The quantification limit of qPCR was defined as fluorescence C_T numbers well within those of the simultaneously run standard curve and being at least 3 values below the nontemplate control C_T. Gene copy numbers were converted into gene copies per gram of fresh sediment by accounting for how much sediment was used for each extraction. For each depth within each core, two technical replicates were performed. To test for association between average copy number and sediment depth, linear models and Spearman's rho were calculated in R using lm(Average ~ Depth) and cor.test, respectively.

16S rRNA gene libraries. Taxonomic diversity of Svalbard sediments was evaluated using 16S rRNA gene library sequencing. Genomic DNA extracts from AB.1, AB.2, AC.1, and AC.2 were used to generate 16S rRNA amplicon libraries (extracts from HA were not amplifiable). Phusion master mix (Thermo Fisher) was used with primer set 515F/806R (97) at the Center for Environmental Biology at The University of Tennessee, Knoxville, for amplification. Reads were sequenced with Illumina MiSeq and trimmed for quality with Trimmomatic using a window 10 bp wide and a minimum phred score of 28 (98). Trimmed reads were then processed in mothur 1.35.1 (99) using the computational cluster at the Bioinformatics Resource Facility at The University of Tennessee, Knoxville. OTUs were clustered *de novo* at the 97% similarity level with the SILVA release 123 (100). Rarefaction analysis was calculated in mothur with rarefaction.single, and reads were normalized with normalize.shared (norm = 60,000).

Ordination analysis was conducted using a combination of Phyloseq (101) and the vegan package in R. NMDS ordination was built using the Bray-Curtis distance metric for 52 samples that had libraries large enough for comparison (Table S4). Geochemical vectors were fit with envfit, and the best parameters to explain the model were determined with bioenv using Spearman correlation and the manhattan metric of Bray-Curtis dissimilarity. Marginal effects of these parameters were determined with dbrda() with a significance cutoff (alpha) of 0.05.

Hydrogen. Samples for hydrogen analysis consisted of 1 ml of sediment placed into a dark glass serum vial which was then crimp sealed and gassed with N_2 for 15 min prior to storage at 4°C. Headspace

was measured with glass syringes on a Peak Performer gas chromatograph (GC) with mercuric chloride detector (Peak Laboratories, Mountain View, CA) at The University of Tennessee, Knoxville, after 4 to 7 days.

Microbial network analysis. To evaluate the co-correlation of target OTUs, we generated microbial networks using relative abundance at the OTU level from all four cores with the Pearson correlation coefficient calculated in the extended local similarity analysis (eLSA) program (102, 103). While abundance measures with 16S rRNA genes are likely not true measures of total abundance, as primer bias can underrepresent or overrepresent specific sequences (104), relative sequence abundance may still be related to actual abundance *in situ*. Networks excluded OTUs whose sum did not reach 0.1% of reads across all libraries from a core. Percent Z normalization was used in network construction and a strict *P* value cutoff of <0.001 was used to determine statistically significant co-occurrence patterns, which ranged in Pearson's *r* values from -0.95 to 1. At this *P* value, the false-discovery rate, or q-estimation, was 0.

Networks were visualized with Cytoscape 3.5.1 (105). Betweenness was calculated with the Analyze Network module in Cytoscape by treating edges as undirected (106). The randomness of the generated networks was tested through examination of the degree distribution. Degree is a node attribute that is simply the sum of all direct connections involving that node. As random networks are characterized by a degree distribution fitting a Poisson distribution (106), we used a chi square (χ^2) test to determine the goodness of fit between observed and expected degree distributions if originating from a Poisson distribution and found that our networks were not random (107).

Sulfate reduction rates. *In situ* sulfate reduction rates (SRR) were determined via the whole-core injection method (108) in 2.5-cm-wide and ca. 20-cm-long subcores that were taken from a HAPs core. Per 1-cm depth interval, 50 kBq of $[^{35}S]SO_4^{2-}$ was injected through predrilled holes in the coring tube that were sealed with polyurethane-based elastic glue. Whole cores were incubated for 14 to 16 h at 2°C. The incubation was stopped by splicing the core in 1-cm sections and mixing each section with 10 ml of 10% zinc acetate and immediate freezing. Samples were stored at -20°C before radiolabeled total reduced inorganic sulfur (TRIS) was recovered and separated from $[^{35}S]SO_4^{2-}$ using the cold chromium distillation method (109). Radioactivities of the distillate and of sulfate in the sample were analyzed using scintillation counting and sulfate reduction rates were calculated according to the method of Jørgensen (108).

Accession number(s). Raw sequences for all 16S rRNA gene libraries are publicly available in the NCBI database under BioProject PRJNA493859.

SUPPLEMENTAL MATERIAL

Supplemental material for this article may be found at https://doi.org/10.1128/AEM.00949-19.

SUPPLEMENTAL FILE 1, PDF file, 7.1 MB.

ACKNOWLEDGMENTS

This work was primarily supported by a grant from the Simons Foundation (404586 to K.G.L.). Additional funding for field work and supplies was provided by a student research grant from the Explorer's Club (to J.B.), an ERC Advanced Grant (MICROENERGY, grant no. 294200, EU 7th FP), the Danish National Research Foundation (DNRF grant no. 104), and the Danish Council for Independent Research (DFF-7014-00196), postdoctoral fellowships from the U.S. National Science Foundation (EAR-PF1625158 to A.B.M.) and the DFG Research Fellowship (389371177 to K.L.). Computing resources were provided by the Center for Dark Energy Biosphere Investigations (C-DEBI, publication number 476).

We thank Natascha Riedinger for assistance with 510 ICP-MS measurements. We also thank Captain Stig Henningsen and first mate Reidar Sorensen of MS *Farm*. We thank the Alfred Wegener Institute—Institute Paul Emile Victor (AWIPEV) station and staff for housing and excellent logistics support. The Polar Geospatial Center and Brad Herried provided geospatial support under NSF OPP awards 1043681 and 1559691 and produced maps from ESA remote sensing data. We thank all the participants of the 2016 Svalbard KOP 56/RiS 10528 expedition for help with sample collection.

REFERENCES

1. Stroeve J, Holland MM, Meier W, Scambos T, Serreze M. 2007. Arctic sea ice decline: faster than forecast. Geophys Res Lett 34:L09501. https://doi.org/10.1029/2007GL029703.
2. Johannessen OM, Bengtsson L, Miles MW, Kuzmina SI, Semenov VA, Alekseev GV, Nagurnyi AP, Zakharov VF, Bobylev LP, Pettersson LH, Hasselmann K, Cattle HP. 2004. Arctic climate change: observed and modelled temperature and sea-ice variability. Tellus A 56:328–341. https://doi.org/10.1111/j.1600-0870.2004.00060.x.
3. Kohler J, James T, Murray T, Nuth C, Brandt O, Barrand N, Aas H, Luckman A. 2007. Acceleration in thinning rate on western Svalbard glaciers. Geophys Res Lett 34:L18502. https://doi.org/10.1029/2007GL030681.
4. Lefauconnier B, Hagen JO, Rudant JP. 1994. Flow speed and calving

rate of Kongsbreen glacier, Svalbard, using SPOT images. Polar Res 13:59–65. https://doi.org/10.1111/j.1751-8369.1994.tb00437.x.
5. Bradley JA, Singarayer JS, Anesio AM. 2014. Microbial community dynamics in the forefield of glaciers. Proc Soc Biol 281:20140882. https://doi.org/10.1098/rspb.2014.0882.
6. Jeffries M, Richter-Menge J, Overland J. 2015. Arctic report card 2015. Arctic Program, NOAA, Washington, DC.
7. Bhatia MP, Kujawinski EB, Das SB, Breier CF, Henderson PB, Charette MA. 2013. Greenland meltwater as a significant and potentially bioavailable source of iron to the ocean. Nat Geosci 6:274. https://doi.org/10.1038/ngeo1746.
8. Coale KH, Johnson KS, Fitzwater SE, Gordon RM, Tanner S, Chavez FP, Ferioli L, Sakamoto C, Rogers P, Millero F, Steinberg P, Nightingale P, Cooper D, Cochlan WP, Landry MR, Constantinou J, Rollwagen G, Trasvina A, Kudela R. 1996. A massive phytoplankton bloom induced by an ecosystem-scale iron fertilization experiment in the equatorial Pacific Ocean. Nature 383:495. https://doi.org/10.1038/383495a0.
9. Falkowski PG, Barber RT, Smetacek V. 1998. Biogeochemical controls and feedbacks on ocean primary production. Science 281:200–206. https://doi.org/10.1126/science.281.5374.200.
10. Anderson LG, Kaltin S. 2001. Carbon fluxes in the Arctic Ocean—potential impact by climate change. Polar Res 20:225–232. https://doi.org/10.3402/polar.v20i2.6521.
11. Walsh JJ. 1989. Arctic carbon sinks: present and future. Glob Biogeochem Cycles 3:393–411. https://doi.org/10.1029/GB003i004p00393.
12. Pabi S, van Dijken GL, Arrigo KR. 2008. Primary production in the Arctic Ocean, 1998–2006. J Geophys Res Oceans 113:1998–2006. https://doi.org/10.1029/2007JC004578.
13. Zhang R, John SG, Zhang J, Ren J, Wu Y, Zhu Z, Liu S, Zhu X, Marsay CM, Wenger F. 2015. Transport and reaction of iron and iron stable isotopes in glacial meltwaters on Svalbard near Kongsfjorden: from rivers to estuary to ocean. Earth Planet Sci Lett 424:201–211. https://doi.org/10.1016/j.epsl.2015.05.031.
14. Wehrmann LM, Formolo MJ, Owens JD, Raiswell R, Ferdelman TG, Riedinger N, Lyons TW. 2014. Iron and manganese speciation and cycling in glacially influenced high-latitude fjord sediments (West Spitsbergen, Svalbard): evidence for a benthic recycling-transport mechanism. Geochim Cosmochim Acta 141:628–655. https://doi.org/10.1016/j.gca.2014.06.007.
15. Wehrmann LM, Riedinger N, Brunner B, Kamyshny A, Jr, Hubert CR, Herbert LC, Brüchert V, Jørgensen BB, Ferdelman TG, Formolo MJ. 2017. Iron-controlled oxidative sulfur cycling recorded in the distribution and isotopic composition of sulfur species in glacially influenced fjord sediments of west Svalbard. Chem Geol 466:678–695. https://doi.org/10.1016/j.chemgeo.2017.06.013.
16. Thamdrup B. 2000. Bacterial manganese and iron reduction in aquatic sediments. Adv Microb Ecol 16:41–84. https://doi.org/10.1007/978-1-4615-4187-5_2.
17. Canfield DE, Thamdrup B, Hansen JW. 1993. The anaerobic degradation of organic matter in Danish coastal sediments: iron reduction, manganese reduction, and sulfate reduction. Geochim Cosmochim Acta 57:3867–3883. https://doi.org/10.1016/0016-7037(93)90340-3.
18. Jørgensen BB. 1982. Mineralization of organic matter in the sea bed—the role of sulphate reduction. Nature 296:643–645. https://doi.org/10.1038/296643a0.
19. Lovley DR, Phillips EJ. 1988. Novel mode of microbial energy metabolism: organic carbon oxidation coupled to dissimilatory reduction of iron or manganese. Appl Environ Microbiol 54:1472–1480.
20. Capone DG, Kiene RP. 1988. Comparison of microbial dynamics in marine and freshwater sediments: contrasts in anaerobic carbon catabolism. Limnol Oceanogr 33:725–749. https://doi.org/10.4319/lo.1988.33.4_part_2.0725.
21. Schippers A, Jørgensen BB. 2002. Biogeochemistry of pyrite and iron sulfide oxidation in marine sediments. Geochim Cosmochim Acta 66:85–92. https://doi.org/10.1016/S0016-7037(01)00745-1.
22. Hop H, Pearson T, Hegseth EN, Kovacs KM, Wiencke C, Kwasniewski S, Eiane K, Mehlum F, Gulliksen B, Wlodarska-Kowalczuk M, Lydersen C, Weslawski JM, Cochrane S, Gabrielsen GW, Leakey RJG, Lønne OJ, Zajaczkowski M, Falk-Petersen S, Kendall M, Wängberg S-Å, Bischof K, Voronkov AY, Kovaltchouk NA, Wiktor J, Poltermann M, Prisco G, Papucci C, Gerland S. 2002. The marine ecosystem of Kongsfjorden, Svalbard. Polar Res 21:167–208. https://doi.org/10.1111/j.1751-8369.2002.tb00073.x.
23. van de Velde S, Meysman FJ. 2016. The influence of bioturbation on iron and sulphur cycling in marine sediments: a model analysis. Aquat Geochem 22:469–504. https://doi.org/10.1007/s10498-016-9301-7.
24. Emerson D, Fleming EJ, McBeth JM. 2010. Iron-oxidizing bacteria: an environmental and genomic perspective. Annu Rev Microbiol 64:561–583. https://doi.org/10.1146/annurev.micro.112408.134208.
25. Arnosti C, Jørgensen B, Sagemann J, Thamdrup B. 1998. Temperature dependence of microbial degradation of organic matter in marine sediments: polysaccharide hydrolysis, oxygen consumption, and sulfate reduction. Mar Ecol Prog Ser 165:59–70. https://doi.org/10.3354/meps165059.
26. Sahm K, Berninger U-G. 1998. Abundance, vertical distribution, and community structure of benthic prokaryotes from permanently cold marine sediments (Svalbard, Arctic Ocean). Mar Ecol Prog Ser 165:71–80. https://doi.org/10.3354/meps165071.
27. Kostka JE, Thamdrup B, Glud RN, Canfield DE. 1999. Rates and pathways of carbon oxidation in permanently cold Arctic sediments. Mar Ecol Prog Ser 180:7–21. https://doi.org/10.3354/meps180007.
28. Knoblauch C, Jørgensen BB, Harder J. 1999. Community size and metabolic rates of psychrophilic sulfate-reducing bacteria in Arctic marine sediments. Appl Environ Microbiol 65:4230–4233.
29. Sagemann J, Jørgensen B, Greeff O. 1998. Temperature dependence and rates of sulfate reduction in cold sediments of Svalbard, Arctic Ocean. Geomicrobiol J 15:85–100. https://doi.org/10.1080/01490459809378067.
30. Ravenschlag K, Sahm K, Pernthaler J, Amann R. 1999. High bacterial diversity in permanently cold marine sediments. Appl Environ Microbiol 65:3982–3989.
31. Vandieken V, Finke N, Jørgensen BB. 2006. Pathways of carbon oxidation in an Arctic fjord sediment (Svalbard) and isolation of psychrophilic and psychrotolerant Fe(III)-reducing bacteria. Mar Ecol Prog Ser 322:29–41. https://doi.org/10.3354/meps322029.
32. Teske A, Durbin A, Ziervogel K, Cox C, Arnosti C. 2011. Microbial community composition and function in permanently cold seawater and sediments from an Arctic fjord of Svalbard. Appl Environ Microbiol 77:2008–2018. https://doi.org/10.1128/AEM.01507-10.
33. Cardman Z, Arnosti C, Durbin A, Ziervogel K, Cox C, Steen A, Teske A. 2014. Verrucomicrobia are candidates for polysaccharide-degrading bacterioplankton in an Arctic fjord of Svalbard. Appl Environ Microbiol 80:3749–3756. https://doi.org/10.1128/AEM.00899-14.
34. Ritchie JC, McHenry JR. 1990. Application of radioactive fallout cesium-137 for measuring soil erosion and sediment accumulation rates and patterns: a review. J Environ Qual 19:215–233. https://doi.org/10.2134/jeq1990.00472425001900020006x.
35. Sund M, Lauknes T, Eiken T. 2014. Surge dynamics in the Nathorstbreen glacier system, Svalbard. Cryosphere 8:623–638. https://doi.org/10.5194/tc-8-623-2014.
36. Kempf P, Forwick M, Laberg JS, Vorren TO. 2013. Late Weichselian and Holocene sedimentary palaeoenvironment and glacial activity in the high-Arctic Van Keulenfjorden, Spitsbergen. Holocene 23:1607–1618. https://doi.org/10.1177/0959683613499055.
37. Winkelmann D, Knies J. 2005. Recent distribution and accumulation of organic carbon on the continental margin west off Spitsbergen. Geochem Geophys Geosyst 6:Q09012. https://doi.org/10.1029/2005GC000916.
38. Kim J-H, Peterse F, Willmott V, Kristensen DK, Baas M, Schouten S, Sinninghe Damsté J. 2011. Large ancient organic matter contributions to Arctic marine sediments (Svalbard). Limnol Oceanogr 56:1463–1474. https://doi.org/10.4319/lo.2011.56.4.1463.
39. O'Leary MH. 1988. Carbon isotopes in photosynthesis. Bioscience 38:328–336. https://doi.org/10.2307/1310735.
40. McMahon KW, Ambrose WG, Jr, Johnson BJ, Sun M-Y, Lopez GR, Clough LM, Carroll ML. 2006. Benthic community response to ice algae and phytoplankton in Ny Ålesund, Svalbard. Mar Ecol Prog Ser 310:1–14. https://doi.org/10.3354/meps310001.
41. Lehmann MF, Bernasconi SM, Barbieri A, McKenzie JA. 2002. Preservation of organic matter and alteration of its carbon and nitrogen isotope composition during simulated and in situ early sedimentary diagenesis. Geochim Cosmochim Acta 66:3573–3584. https://doi.org/10.1016/S0016-7037(02)00968-7.
42. Llobet-Brossa E, Rosselló-Mora R, Amann R. 1998. Microbial community composition of Wadden Sea sediments as revealed by fluorescence in situ hybridization. Appl Environ Microbiol 64:2691–2696.
43. Ishii K, Mussmann M, MacGregor BJ, Amann R. 2004. An improved fluorescence in situ hybridization protocol for the identification of

bacteria and archaea in marine sediments. FEMS Microbiol Ecol 50:203–213. https://doi.org/10.1016/j.femsec.2004.06.015.
44. Lloyd KG, May MK, Kevorkian RT, Steen AD. 2013. Meta-analysis of quantification methods shows that archaea and bacteria have similar abundances in the subseafloor. Appl Environ Microbiol 79:7790–7799. https://doi.org/10.1128/AEM.02090-13.
45. Buongiorno J, Turner S, Webster G, Asai M, Shumaker AK, Roy T, Weightman A, Schippers A, Lloyd KG. 2017. Interlaboratory quantification of Bacteria and Archaea in deeply buried sediments of the Baltic Sea (IODP Expedition 347). FEMS Microbiol Ecol 93:fix007. https://doi.org/10.1093/femsec/fix007.
46. Kubo K, Lloyd KG, Biddle JF, Amann R, Teske A, Knittel K. 2012. Archaea of the Miscellaneous Crenarchaeotal Group are abundant, diverse and widespread in marine sediments. ISME J 6:1949–1965. https://doi.org/10.1038/ismej.2012.37.
47. Dowdeswell JA, Cromack M. 1991. Behavior of a glacier-derived suspended sediment plume in a small Arctic inlet. J Geol 99:111–123. https://doi.org/10.1086/629477.
48. Jørgensen BB, Glud RN, Holby O. 2005. Oxygen distribution and bioirrigation in Arctic fjord sediments (Svalbard, Barents Sea). Mar Ecol Prog Ser 292:85–95. https://doi.org/10.3354/meps292085.
49. Ravenschlag K, Sahm K, Knoblauch C, Jørgensen BB, Amann R. 2000. Community structure, cellular rRNA content, and activity of sulfate-reducing bacteria in marine arctic sediments. Appl Environ Microbiol 66:3592–3602. https://doi.org/10.1128/AEM.66.8.3592-3602.2000.
50. Platen H, Temmes A, Schink B. 1990. Anaerobic degradation of acetone by Desulfococcus biacutus spec. nov. Arch Microbiol 154:355–361. https://doi.org/10.1007/BF00276531.
51. Harms G, Zengler K, Rabus R, Aeckersberg F, Minz D, Rosselló-Mora R, Widdel F. 1999. Anaerobic oxidation of o-xylene, m-xylene, and homologous alkylbenzenes by new types of sulfate-reducing bacteria. Appl Environ Microbiol 65:999–1004.
52. Evans WC, Fuchs G. 1988. Anaerobic degradation of aromatic compounds. Annu Rev Microbiol 42:289–317. https://doi.org/10.1146/annurev.mi.42.100188.001445.
53. Dagley S. 1971. Catabolism of aromatic compounds by microorganisms. Adv Microb Physiol 6:1–46. https://doi.org/10.1016/S0065-2911(08)60066-1.
54. Rabus R, Nordhaus R, Ludwig W, Widdel F. 1993. Complete oxidation of toluene under strictly anoxic conditions by a new sulfate-reducing bacterium. Appl Environ Microbiol 59:1444–1451.
55. Imhoff-Stuckle D, Pfennig N. 1983. Isolation and characterization of a nicotinic acid-degrading sulfate-reducing bacterium, Desulfococcus niacini sp. nov. Arch Microbiol 136:194–198. https://doi.org/10.1007/BF00409843.
56. Dyksma S, Pjevac P, Ovanesov K, Mussmann M. 2018. Evidence for H_2 consumption by uncultured Desulfobacterales in coastal sediments. Environ Microbiol 20:450–461. https://doi.org/10.1111/1462-2920.13880.
57. Holmes DE, Nicoll JS, Bond DR, Lovley DR. 2004. Potential role of a novel psychrotolerant member of the family Geobacteraceae, *Geopsychrobacter electrodiphilus* gen. nov., sp. nov., in electricity production by a marine sediment fuel cell. Appl Environ Microbiol 70:6023–6030. https://doi.org/10.1128/AEM.70.10.6023-6030.2004.
58. Prakash O, Gihring TM, Dalton DD, Chin K-J, Green SJ, Akob DM, Wanger G, Kostka JE. 2010. *Geobacter daltonii* sp. nov., an Fe(III)- and uranium(VI)-reducing bacterium isolated from a shallow subsurface exposed to mixed heavy metal and hydrocarbon contamination. Int J Syst Evol Microbiol 60:546–553. https://doi.org/10.1099/ijs.0.010843-0.
59. Enning D, Venzlaff H, Garrelfs J, Dinh HT, Meyer V, Mayrhofer K, Hassel AW, Stratmann M, Widdel F. 2012. Marine sulfate-reducing bacteria cause serious corrosion of iron under electroconductive biogenic mineral crust. Environ Microbiol 14:1772–1787. https://doi.org/10.1111/j.1462-2920.2012.02778.x.
60. Froelich PN, Klinkhammer GP, Bender ML, Luedtke NA, Heath GR, Cullen D, Dauphin P, Hammond D, Hartman B, Maynard V. 1979. Early oxidation of organic matter in pelagic sediments of the eastern equatorial Atlantic: suboxic diagenesis. Geochim Cosmochim Acta 43:1075–1090. https://doi.org/10.1016/0016-7037(79)90095-4.
61. Orcutt BN, Sylvan JB, Knab NJ, Edwards KJ. 2011. Microbial ecology of the dark ocean above, at, and below the seafloor. Microbiol Mol Biol Rev 75:361–422. https://doi.org/10.1128/MMBR.00039-10.
62. Otte JM, Harter J, Laufer K, Blackwell N, Straub D, Kappler A, Kleindienst S. 2018. The distribution of active iron-cycling bacteria in marine and freshwater sediments is decoupled from geochemical gradients. Environ Microbiol 20:2483–2499. https://doi.org/10.1111/1462-2920.14260.
63. Liesack W, Finster K. 1994. Phylogenetic analysis of five strains of gram-negative, obligately anaerobic, sulfur-reducing bacteria and description of Desulfuromusa gen. nov., including Desulfuromusa kysingii sp. nov., Desulfuromusa bakii sp. nov., and Desulfuromusa succinoxidans sp. nov. Int J Syst Evol Microbiol 44:753–758. https://doi.org/10.1099/00207713-44-4-753.
64. Holmes DE, Bond DR, Lovley DR. 2004. Electron transfer by *Desulfobulbus propionicus* to Fe(III) and graphite electrodes. Appl Environ Microbiol 70:1234–1237. https://doi.org/10.1128/AEM.70.2.1234-1237.2004.
65. Fuseler K, Cypionka H. 1995. Elemental sulfur as an intermediate of sulfide oxidation with oxygen by Desulfobulbus propionicus. Arch Microbiol 164:104–109. https://doi.org/10.1007/BF02525315.
66. Fuseler K, Krekeler D, Sydow U, Cypionka H. 1996. A common pathway of sulfide oxidation by sulfate-reducing bacteria. FEMS Microbiol Lett 144:129–134. https://doi.org/10.1111/j.1574-6968.1996.tb08518.x.
67. Sorokin DY, Tourova TP, Panteleeva AN, Muyzer G. 2012. *Desulfonatronobacter acidivorans* gen. nov., sp. nov. and *Desulfobulbus alkaliphilus* sp. nov., haloalkaliphilic heterotrophic sulfate-reducing bacteria from soda lakes. Int J Syst Evol Microbiol 62:2107–2113. https://doi.org/10.1099/ijs.0.029777-0.
68. Coates JD, Lonergan DJ, Philips EJP, Jenter H, Lovley DR. 1995. *Desulfuromonas palmitatis* sp. nov., a marine dissimilatory Fe(III) reducer that can oxidize long-chain fatty acids. Arch Microbiol 164:406–413. https://doi.org/10.1007/s002030050282.
69. Inagaki F, Takai K, Nealson KH, Horikoshi K. 2004. *Sulfurovum lithotrophicum* gen. nov., sp. nov., a novel sulfur-oxidizing chemolithoautotroph within the ε-Proteobacteria isolated from Okinawa Trough hydrothermal sediments. Int J Syst Evol Microbiol 54:1477–1482. https://doi.org/10.1099/ijs.0.03042-0.
70. Tanaka N, Romanenko LA, Iino T, Frolova GM, Mikhailov VV. 2011. *Cocleimonas flava* gen. nov., sp. nov., a gammaproteobacterium isolated from sand snail (Umbonium costatum). Int J Syst Evol Microbiol 61:412–416. https://doi.org/10.1099/ijs.0.020263-0.
71. Berg P, Rysgaard S, Thamdrup B. 2003. Dynamic modeling of early diagenesis and nutrient cycling. A case study in an artic marine sediment. Am J Sci 303:905–955. https://doi.org/10.2475/ajs.303.10.905.
72. Singer E, Emerson D, Webb EA, Barco RA, Kuenen JG, Nelson WC, Chan CS, Comolli LR, Ferriera S, Johnson J, Heidelberg JF, Edwards KJ. 2011. *Mariprofundus ferrooxydans* PV-1 the first genome of a marine Fe(II) oxidizing zetaproteobacterium. PLoS One 6:e25386. https://doi.org/10.1371/journal.pone.0025386.
73. Makita H, Tanaka E, Mitsunobu S, Miyazaki M, Nunoura T, Uematsu K, Takaki Y, Nishi S, Shimamura S, Takai K. 2017. *Mariprofundus micogutta* sp. nov., a novel iron-oxidizing zetaproteobacterium isolated from a deep-sea hydrothermal field at the Bayonnaise knoll of the Izu-Ogasawara arc, and a description of Mariprofundales ord. nov. and Zetaproteobacteria classis nov. Arch Microbiol 199:335–346. https://doi.org/10.1007/s00203-016-1307-4.
74. Scott JJ, Breier JA, Luther GW, III, Emerson D. 2015. Microbial iron mats at the Mid-Atlantic Ridge and evidence that Zetaproteobacteria may be restricted to iron-oxidizing marine systems. PLoS One 10:e0119284. https://doi.org/10.1371/journal.pone.0119284.
75. McBeth JM, Fleming EJ, Emerson D. 2013. The transition from freshwater to marine iron-oxidizing bacterial lineages along a salinity gradient on the Sheepscot River, Maine, USA. Environ Microbiol Rep 5:453–463. https://doi.org/10.1111/1758-2229.12033.
76. Fuhrman JA. 2009. Microbial community structure and its functional implications. Nature 459:193–199. https://doi.org/10.1038/nature08058.
77. Berry D, Widder S. 2014. Deciphering microbial interactions and detecting keystone species with co-occurrence networks. Front Microbiol 5:219. https://doi.org/10.3389/fmicb.2014.00219.
78. Loveless J, Painter H. 1968. The influence of metal ion concentrations and pH value on the growth of a Nitrosomonas strain isolated from activated sludge. Microbiology 52:1–14. https://doi.org/10.1099/00221287-52-1-1.
79. Li J, Nedwell DB, Beddow J, Dumbrell AJ, McKew BA, Thorpe EL, Whitby C. 2015. *amoA* gene abundances and nitrification potential rates suggest that benthic ammonia-oxidizing bacteria and not archaea dominate N cycling in the Colne Estuary, United Kingdom. Appl Environ Microbiol 81:159–165. https://doi.org/10.1128/AEM.02654-14.
80. Hansen JI, Henriksen K, Blackburn TH. 1981. Seasonal distribution of

nitrifying bacteria and rates of nitrification in coastal marine sediments. Microb Ecol 7:297–304. https://doi.org/10.1007/BF02341424.
81. Wankel SD, Mosier AC, Hansel CM, Paytan A, Francis CA. 2011. Spatial variability in nitrification rates and ammonia-oxidizing microbial communities in the agriculturally impacted Elkhorn Slough Estuary, California. Appl Environ Microbiol 77:269–280. https://doi.org/10.1128/AEM.01318-10.
82. Barrat A, Barthelemy M, Pastor-Satorras R, Vespignani A. 2004. The architecture of complex weighted networks. Proc Natl Acad Sci U S A 101:3747–3752. https://doi.org/10.1073/pnas.0400087101.
83. Drakare S. 2002. Competition between picoplanktonic cyanobacteria and heterotrophic bacteria along crossed gradients of glucose and phosphate. Microb Ecol 44:327–335. https://doi.org/10.1007/s00248-002-1013-4.
84. Pande S, Shitut S, Freund L, Westermann M, Bertels F, Colesie C, Bischofs IB, Kost C. 2015. Metabolic cross-feeding via intercellular nanotubes among bacteria. Nat Commun 6:6238. https://doi.org/10.1038/ncomms7238.
85. Kanneworff E, Nicolaisen W. 1972. The "Haps" a frame-supported bottom corer. Ophelia 10:119–128. https://doi.org/10.1080/00785326.1972.10430108.
86. Huntley SL, Wenning RJ, Su SH, Bonnevie NL, Paustenbach DJ. 1995. Geochronology and sedimentology of the lower Passaic River, New Jersey. Estuaries Coast 18:351–361. https://doi.org/10.2307/1352317.
87. Winkels H, Kroonenberg S, Lychagin MY, Marin G, Rusakov G, Kasimov N. 1998. Geochronology of priority pollutants in sedimentation zones of the Volga and Danube delta in comparison with the Rhine delta. Appl Geochem 13:581–591. https://doi.org/10.1016/S0883-2927(98)00002-X.
88. Valero-Garcés BL, Navas A, Machín J, Walling D. 1999. Sediment sources and siltation in mountain reservoirs: a case study from the Central Spanish Pyrenees. Geomorphology 28:23–41. https://doi.org/10.1016/S0169-555X(98)00096-8.
89. Dickens GR, Koelling M, Smith DC, Schnieders L. 2007. Rhizon sampling of pore waters on scientific drilling expeditions: an example from the IODP Expedition 302, Arctic Coring Expedition (ACEX). Sci Drilling 4:22–25. https://doi.org/10.5194/sd-4-22-2007.
90. Seeberg-Elverfeldt J, Schlüter M, Feseker T, Kölling MJL. 2005. Rhizon sampling of porewaters near the sediment-water interface of aquatic systems. Limnol Oceanogr Methods 3:361–371. https://doi.org/10.4319/lom.2005.3.361.
91. Harris D, Horwáth WR, Van Kessel C. 2001. Acid fumigation of soils to remove carbonates prior to total organic carbon or carbon-13 isotopic analysis. Soil Sci Soc Am J 65:1853–1856. https://doi.org/10.2136/sssaj2001.1853.
92. Cook RD. 1979. Influential observations in linear regression. J Am Stat Assoc 74:169–174. https://doi.org/10.2307/2286747.
93. R Core Team. 2015. R: a language and environment for statistical computing. R Foundation for Statistical Computing, Vienna, Austria.
94. Nadkarni MA, Martin FE, Jacques NA, Hunter N. 2002. Determination of bacterial load by real-time PCR using a broad-range (universal) probe and primers set. Microbiology 148:257–266. https://doi.org/10.1099/00221287-148-1-257.
95. Takai K, Horikoshi K. 2000. Rapid detection and quantification of members of the archaeal community by quantitative PCR using fluorogenic probes. Appl Environ Microbiol 66:5066–5072. https://doi.org/10.1128/AEM.66.11.5066-5072.2000.
96. Stahl DA, Amann R. 1991. Development and application of nucleic acid probes, p 205–248. *In* Stackebrandt E, Goodfellow M (ed), Nucleic acid techniques in bacterial systems. John Wiley and Sons Ltd, Chichester, United Kingdom.
97. Caporaso JG, Lauber CL, Walters WA, Berg-Lyons D, Lozupone CA, Turnbaugh PJ, Fierer N, Knight R. 2011. Global patterns of 16S rRNA diversity at a depth of millions of sequences per sample. Proc Natl Acad Sci U S A 108:4516–4522. https://doi.org/10.1073/pnas.1000080107.
98. Bolger AM, Lohse M, Usadel B. 2014. Trimmomatic: a flexible trimmer for Illumina sequence data. Bioinformatics 30:2114–2120. https://doi.org/10.1093/bioinformatics/btu170.
99. Schloss PD, Westcott SL, Ryabin T, Hall JR, Hartmann M, Hollister EB, Lesniewski RA, Oakley BB, Parks DH, Robinson CJ, Sahl JW, Stres B, Thallinger GG, Van Horn DJ, Weber CF. 2009. Introducing mothur: open-source, platform-independent, community-supported software for describing and comparing microbial communities. Appl Environ Microbiol 75:7537–7541. https://doi.org/10.1128/AEM.01541-09.
100. Pruesse E, Peplies J, Glöckner FO. 2012. SINA: accurate high-throughput multiple sequence alignment of ribosomal RNA genes. Bioinformatics 28:1823–1829. https://doi.org/10.1093/bioinformatics/bts252.
101. McMurdie PJ, Holmes S. 2013. phyloseq: an R package for reproducible interactive analysis and graphics of microbiome census data. PLoS One 8:e61217. https://doi.org/10.1371/journal.pone.0061217.
102. Xia LC, Ai D, Cram J, Fuhrman JA, Sun F. 2013. Efficient statistical significance approximation for local similarity analysis of high-throughput time series data. Bioinformatics 29:230–237. https://doi.org/10.1093/bioinformatics/bts668.
103. Xia LC, Steele JA, Cram JA, Cardon ZG, Simmons SL, Vallino JJ, Fuhrman JA, Sun F. 2011. Extended local similarity analysis (eLSA) of microbial community and other time series data with replicates. BMC Syst Biol 5:S15. https://doi.org/10.1186/1752-0509-5-S2-S15.
104. Parada AE, Needham DM, Fuhrman JA. 2016. Every base matters: assessing small subunit rRNA primers for marine microbiomes with mock communities, time series and global field samples. Environ Microbiol 18:1403–1414. https://doi.org/10.1111/1462-2920.13023.
105. Shannon P, Markiel A, Ozier O, Baliga NS, Wang JT, Ramage D, Amin N, Schwikowski B, Ideker T. 2003. Cytoscape: a software environment for integrated models of biomolecular interaction networks. Genome Res 13:2498–2504. https://doi.org/10.1101/gr.1239303.
106. Assenov Y, Ramírez F, Schelhorn S-E, Lengauer T, Albrecht M. 2008. Computing topological parameters of biological networks. Bioinformatics 24:282–284. https://doi.org/10.1093/bioinformatics/btm554.
107. Wasserman S, Faust K. 1994. Social network analysis: methods and applications, vol 8. Cambridge University Press, Cambridge, United Kingdom.
108. Jørgensen BB. 1978. A comparison of methods for the quantification of bacterial sulfate reduction in coastal marine sediments. Geomicrobiology J 1:49–64. https://doi.org/10.1080/01490457809377723.
109. Røy H, Weber HS, Tarpgaard IH, Ferdelman TG, Jørgensen BB. 2014. Determination of dissimilatory sulfate reduction rates in marine sediment via radioactive ^{35}S tracer. Limnol Oceanogr Methods 12:196–211. https://doi.org/10.4319/lom.2014.12.196.